

Practical approach to calculating the hydrodynamic oscillating loads of a ship propeller under non-uniform wake field

Hassan Ghassemi

Amirkabir University of Technology (AUT), Department of Maritime Engineering
Hafez Ave, No. 424, P.O. Box 15875-4413, Tehran, Iran
e-mail: gasemi@aut.ac.ir



Hassan Ghassemi works at the Maritime Engineering Department, Amirkabir University of Technology (AUT). He completed his post-graduate education in Poland, Japan and Canada between 1990 and 2000. His major field of study is marine hydrodynamics, propulsor, ship design and numerical methods. He has published more than 120 journal papers and 6 books. He has prepared ship propeller design (SPD) software and employed it to the design of a ship's propeller. He is editorial member of more than 10 international journals. Currently, he is a full professor at AUT with 18 years educational and research experiences.

Key words: hydrodynamic performance, non-uniform wake, oscillating thrust and torque, practical approach, ship propeller, ship design

Abstract

Propellers usually operate in the ship's stern, where the inflow of the non-uniform wake generates oscillating loads and changes the hydrodynamic performance. Therefore, determination of the forces on propellers and hydrodynamic performance due to a non-uniform wake field are the challenging problems for naval architects and hydrodynamicists. The main objectives of the present study are to assess the hydrodynamic performance for a single blade and all the blades. The propeller is a B-series propeller under non-uniform wake field behind the Seiun-Maru (hereafter SM) ship hull. A practical approach is employed to calculate the hydrodynamic oscillating loads of the ship propeller under a non-uniform wake field. Results of the computations on the propeller behind the SM ship, due to a non-uniform wake field, are presented and analyzed using classical mathematical methods over a single cycle. The results show that a variation of thrust with the discussed parameters is the same as that shown for torque, also the blade-frequency of the total force, thrust and torque is an increasing function of radial sections, whereas these parameters decrease with increasing radial blade sections.

Introduction

Marine propellers are essential part of the ship propulsion systems. Propellers due to their operational position at the ship stern are under the effects of a non-uniform wake. This wake leads to fluctuating loads on the propeller, which may be induced towards the ship's hull. Moreover, the performance

of propellers may be affected by this non-uniform wake. Indeed, inflows wake regime entry to propellers has a major effect on their behavior. The non-uniform wake regime is strongly related to the shape of the ship hull. As a result, prediction of the ship's propeller performance under non-uniform wakes is a necessity to achieve an efficient propeller. Moreover, because of the ship's propeller flow

interaction with non-uniform wake field behind the hull, prediction of the ship's propeller performance under the non-uniform wake is a great challenge for scholars.

Kamarlouei et al. (Kamarlouei et al., 2014) presented a computational method to estimate the hydrodynamic performance of the minimum cavitation, highest efficiency, and the acceptable blade strength using multi-objective evolutionary optimization technique. The included parameters were the number of blades, chord length, thickness, camber, pitch, diameter, and skew. Gaafary et al. (Gaafary, El-Kilani & Moustafa, 2011) introduced a procedure to find out the optimum characteristics of B-series marine propellers. In this research, the propeller design process is performed as a single objective function subjected to constraints imposed by cavitation, material strength and required propeller thrust. Taheri and Mazaheri (Taheri & Mazaheri, 2013) developed a propeller design method based on a vortex lattice algorithm. They applied a two gradient-based and non-gradient-based optimization algorithm to optimize the shape and efficiency of the two propellers. Szelangiewicz and Abramowski (Abramowski & Szelangiewicz, 2009, 2010; Abramowski, Żelazny & Szelangiewicz, 2010) presented results of numerical calculations of hull resistance, wake, and efficiency of a propeller operating in a non-homogenous velocity field, performed for research on 18 hull versions of a B573 ship designed and built in the Szczecin Nowa Shipyard.

Recently, several studies have reported attempts to calculate a ship hull wakes obtained by experimental tests (Guo et al., 2017; Kleinwächter et al., 2017; Kumar, Nagarajan & Sha, 2017). Also, various experimental and numerical studies are done to investigate ship propeller behavior under inflow wakes. For example, Ghassemi (Ghassemi, 2009) studied the effects of wake and skew on the ship propeller performance by using a boundary element method (BEM). He reported the pressure distribution, open water characteristics and thrust oscillating on a conventional propeller and highly skewed one under two types of non-uniform wakes. Ji et al. (Ji et al., 2012b) simulated the cavitating flow around a marine propeller under a non-uniform inflow wake by Partially Averaged Navier–Stokes (PANS) method. In another study, Ji et al. (Ji et al., 2012a) investigated the excited pressure fluctuation around propellers operating in a non-uniform wake. They conclude that the acceleration due to the cavity volume changes is the main source of the pressure fluctuations. Berger et al. (Berger et al., 2013) designed

a simulation procedure to calculate of wake scale influences on hull pressure fluctuations. They compared the volume acceleration and pressure amplitudes at different scales. Performance of a marine propeller under free wake in an open water condition is evaluated numerically by Greco et al. (Greco et al., 2014). They considered the propeller thrust and torque, slipstream velocities, blade pressure distribution and pressure disturbance to analyze of the performance of a marine propeller by BEM. Shin et al. (Shin, Regener & Andersen, 2015) simulated the unsteady cavitation on a tip-modified propeller under the ship wake fields by using BEM and CFD. They used two types of ship wakes including a model test measurement and bare hull RNAS simulations. Martin et al. (Martin, Michael & Carrica, 2015) investigated the maneuverability of submarines by considering the propeller forces and moments under the hull wake, numerically. They used a coupled CFD/potential flow propeller solver to assess the propeller performance. Abbas et al. (Abbas et al., 2015) simulated the oscillating loads on marine propellers under a non-uniform and non-stationary wake, numerically. They used the hybrid URANS-LES model to predict unsteady loading on a marine propeller behind a KVLCC2 tanker. Moreover, Vaz et al. (Vaz et al., 2015) reported performance characteristics, pressure distributions, limiting-streamlines, and cavitation volumes of the E779A propeller in open water and in a cavitation tunnel behind a non-uniform wake generating plates which are performed by eight different flow codes. Pecoraro et al. (Pecoraro et al., 2006) analyzed the propeller inflow of a single-screw chemical tanker vessel affected by massive flow separation in the stern region. Flow measurements were performed in the propeller region using a scaled model, in the Large Circulating Water Channel of CNR-INSEAN by Laser Doppler Velocimetry (LDV). Tests were undertaken with and without the propeller in order to investigate its effect on the inflow characteristics and the separation mechanisms. Starke et al. (Starke, Windt & Raven, 2006) presented and discussed a full-scale wake field validation for a number of ships. Kadoi et al. (Kadoi, Okamoto & Suzuki, 1980) performed wake surveys both in the towing tank and in a cavitation tunnel using three GeoSim (geometrically similar) ship models, in order to investigate the tunnel wall influence on the wake distributions behind the ship models in the cavitation tunnel. Kim and Moon (Kim & Moon, 2006) applied the neuro-fuzzy technique to estimate the wake field distribution on propeller plane of ship. In this paper the wake distribution

datasets of stern flow fields were collected systematically by model tests of a ship. Also, Calcagno et al. (Calcagno et al., 2002) presented an experimental investigation of a five blade MAU propeller wake behind a Series 60 $C_B = 0.6$ ship model, using Stereo Particle Image Velocimetry (Stereo-PIV) in a large free surface cavitation tunnel.

In the recent years, Pereira et al. (Alves Pereira, Di Felice & Salvatore, 2016) performed an experimental study on a cavitating propeller operating in a non-uniform flow field. They used a wake simulator to create a local flow perturbation upstream of the propeller and suggested quantitative correlations between the near pressure fields and the cavitation pattern. Ueno and Tsukada (Ueno & Tsukada, 2016) perform an experimental study to estimate the fluctuating full-scale propeller torque and thrust, using a free-running model ship in waves and under non-uniform wakes. Sun et al. (Sun et al., 2017) predicted the propeller exciting force under the non-uniform wake of a KCS container ship in oblique flow, numerically. They utilized a hybrid method of RANS and a volume of fluid (VOF) model. In addition, Zou et al. (Zou et al., 2017) conducted a hydro-elastic analysis on the marine propeller under the inflow wakes and the effects of shafts, numerically by using coupled FEM-BEM. Recently, Mahmoodi et al. obtained a mathematical function of the propeller thrust and torque coefficients fluctuations at non-uniform wake flow including geometry effects (Mahmoodi, Ghassemi & Nowruzi, 2018).

According to cited work, the performance and oscillating loads on propellers under the non-uniform wakes is not well-known. Therefore, in the present study, the hydrodynamic performance of oscillating loading of a B-series propeller under non-uniform inflow wake, behind the SM ship hull by classical mathematical methods over one cycle is studied.

The rest of this paper is organized as follows: the first section gives an outline of the mathematical formulations' technique to compute oscillating thrust, torque, and forces. The next section provides some details about propeller and inflow wake data, respectively. After this, the results of computations of the thrust, torque, and forces are presented, and the results are compared and discussed. This is followed by the conclusive remarks in the final section.

Mathematical formulations

In this section a short overview of the formulas utilized to calculate the propeller forces and performance are given. The following formulas have

conventional and well-known forms and, in these formulas, different types of simplifications and approximations are used to estimate the desired quantities.

The velocity into the propeller in Cartesian coordinates is defined by:

$$\vec{V}_w(x, y, z) = V_s(1 - \bar{w}(x, y, z)) \quad (1)$$

And in cylindrical coordinates as follows:

$$\vec{V}_w(x, r, t) = V_s(1 - \bar{w}(x, r, t)) \quad (2)$$

where \vec{V}_w is the non-uniform wake velocity towards the propeller in cylindrical coordinates, which is used to obtain the propeller performance, $\bar{w}(x, r, t)$ denotes the measured non-uniform wake flow, and V_s is the ship speed. The non-uniform wake field is strongly dependent on the ship's stern and on environmental conditions, so each vessel may be considered to have a unique wake field.

The flow into the propeller varies along the circumference at each radius; this phenomenon causes oscillations in thrust and torque, and produces an oscillating load on the propeller blades. Non-uniform flow into the propeller may result in periodic forces and moments, also periodic cavitation causing enhanced vibration, noise, erosion, and fatigue failure. The axial and tangential components of the flow velocity, into the propeller disc, typically vary around the circumference at a given radius. Let V_a , V_t and V_r be the axial, tangential and radial velocities, respectively, and θ be the angle measured from the vertical upward. The nominal wake velocity field including tangential and axial components is represented via a Fourier series. In general, the axial, tangential and radial velocities in the propeller disc can be decomposed into an infinite set of sinusoidal components of various harmonic orders represented in terms of Fourier series, as follows:

$$\begin{cases} V_a(r, \theta) = \sum_{m=0}^{\infty} \{a_m(r) \cos(m\theta) + b_m(r) \sin(m\theta)\} \\ V_r(r, \theta) = \sum_{m=0}^{\infty} \{a'_m(r) \cos(m\theta) + b'_m(r) \sin(m\theta)\} \\ V_t(r, \theta) = \sum_{m=0}^{\infty} \{a''_m(r) \cos(m\theta) + b''_m(r) \sin(m\theta)\} \end{cases} \quad (3)$$

where a_m , a'_m , a''_m and b_m , b'_m , b''_m are Fourier coefficients. In practice, only a limited set of harmonic components are used, typically when $m = 15$ to 20 a reasonably accurate representation to define the

wake field. Similar equations can be defined for the tangential and radial components of the velocity.

The quasi-static approach is a simple method to determine the oscillating propeller forces based on the Fourier series representation of the axial and tangential velocities. This theory neglects all influence of the shed vorticity and the influence of all time-dependent effects on the loading and assumes that the thrust and the moment coefficients are known (K_t, K_Q).

The thrust T and torque Q at the angle θ for all the Z blades are as follows:

$$\begin{cases} T(\theta) = \sum_{i=1}^Z T_i \left[\theta + \frac{2\pi(i-1)}{Z} \right] \\ Q(\theta) = \sum_{i=1}^Z Q_i \left[\theta + \frac{2\pi(i-1)}{Z} \right] \end{cases} \quad (4)$$

where the thrust and torque of the first blade ($i = 1$) at the angle θ are given as:

$$\begin{cases} T_1(\theta) = \frac{1}{Z} K_T(\theta) \rho n^2(\theta) D^4 \\ Q_1(\theta) = \frac{1}{Z} K_Q(\theta) \rho n^2(\theta) D^5 \end{cases} \quad (5)$$

where ρ and D are the density of water and diameter of propeller, respectively. The thrust and torque coefficients ($K_T(\theta)$ and $K_Q(\theta)$) can be obtained from the open water characteristics. Also, $n(\theta)$ is the instantaneous revolution rate at the angle θ :

$$n(\theta) = n - \frac{V_t(\theta)}{X \pi R} \quad (6)$$

where n , R ($= D/2$), and X ($= r/R$) are the rotational speed, propeller radius and non-dimensional radial section, respectively. The advance coefficient for a blade at the angle θ is:

$$J(\theta) = \frac{V_a(\theta)}{n(\theta) D} \quad (7)$$

The mean thrust and torque are determined by integration of the local thrust and torque along the blade span. So, the mean thrust and torque of the propeller are:

$$\begin{cases} T = \frac{1}{2\pi} \int_0^{2\pi} T(\theta) d\theta \\ Q = \frac{1}{2\pi} \int_0^{2\pi} Q(\theta) d\theta \end{cases} \quad (8)$$

For all the Z blades, the tangential force and its horizontal and vertical components are:

$$\begin{cases} F(\theta) = \sum_{i=1}^Z F_i \left[\theta + \frac{2\pi(i-1)}{Z} \right] \\ F_H(\theta) = \sum_{i=1}^Z F_i \left[\theta + \frac{2\pi(i-1)}{Z} \right] \cos \left[\theta + \frac{2\pi(i-1)}{Z} \right] \\ F_V(\theta) = \sum_{i=1}^Z F_i \left[\theta + \frac{2\pi(i-1)}{Z} \right] \sin \left[\theta + \frac{2\pi(i-1)}{Z} \right] \end{cases} \quad (9)$$

It is assumed that the propeller oscillating loading is a linear phenomenon. The tangential force and its horizontal and vertical components at the first blade are:

$$\begin{cases} F_1(\theta) = Q_1(\theta) / r_Q \\ F_{1H}(\theta) = F_1(\theta) \cos(\theta) \\ F_{1V}(\theta) = F_1(\theta) \sin(\theta) \end{cases} \quad (10)$$

where r_Q is the centroid of the tangential force on each blade. The condition for cavitation to occur on a propeller blade section is that the minimum value of pressure coefficient C_p be equal to the local cavitation number. The C_p , for a blade section at a non-dimensional radius $X = r/R$ and angle θ to the upwardly directed vertical line is as follows:

$$-C_{p_{\min}} = \frac{P_A + \rho g(h - XR \cos(\theta)) - P_V}{\frac{1}{2} \rho [V_A^2 + \{2\pi nXR - V_t\}^2]} \quad (11)$$

where P_A and P_V are atmospheric pressure and vapour pressure, h is the depth of immersion of the propeller shaft axis, and g is constant acceleration due to gravity ($P_A = 101$ kPa, $P_V = 2$ kPa, $g = 9.81$ m/s²). The non-dimensional hydrodynamic characteristics of the oscillating propeller are expressed as:

$$\begin{cases} K_t(\theta) = \frac{T(\theta)}{\rho n^2(\theta) D^4} \\ K_Q(\theta) = \frac{Q(\theta)}{\rho n^2(\theta) D^5} \\ \eta(\theta) = \frac{K_t(\theta) J(\theta)}{K_Q(\theta) 2\pi} \end{cases} \quad (12)$$

In the steady calculations, the hydrodynamic characteristics of the propeller are obtained using polynomial regression analysis as given below:

$$\begin{cases} K_t = \frac{T}{\rho n^2 D^4} = \sum_n C_n (J)^{s_n} (P/D)^{t_n} (A_E/A_0)^{u_n} (z)^{v_n} \\ K_Q = \frac{Q}{\rho n^2 D^5} = \sum_n C_n (J)^{s_n} (P/D)^{t_n} (A_E/A_0)^{u_n} (z)^{v_n} \end{cases} \quad (13)$$

The K_t and K_Q parameters are functions of propeller blade number (Z), the blade area ratio (A_E/A_0) and the pitch ratio (P/D). The values of C_n, S_n, t_n, u_n and v_n are regression coefficients (Carlton, 2013).

B-Series Propeller and SM ship wake

In order to evaluate the applicability of the discussed method, a B-series propeller (B:5–0.95) with pitch ratio of 0.9 and 3.6 m in diameter is examined. Figure 1 shows a schematic representation of this propeller.

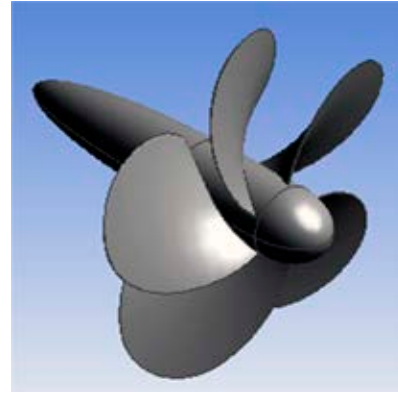


Figure 1. Schematic view of the propeller

The comparison of the open water characteristics of the propeller is presented in Figure 2. The present results are shown in good agreement with the experimental data. With the relative error is found about less than 3 percent at low advance velocity coefficient.

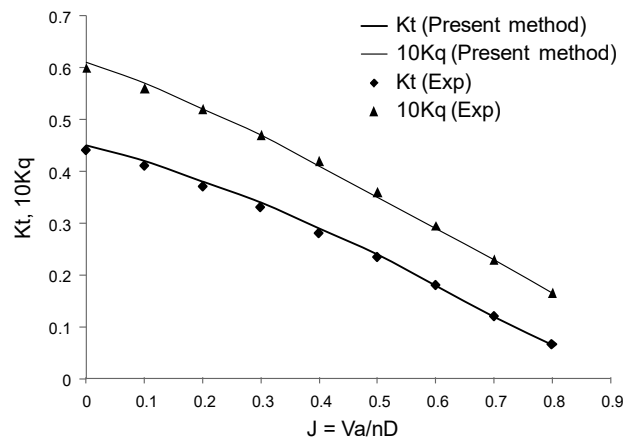


Figure 2. Comparison of the open water characteristics

The inflow of non-uniform SM ship wake is applied to this selected propeller. Contour and vector inflow non-uniform wake velocity distribution and axial, tangential and radial velocity at sixteen radii for SM ship are presented in Figure 3. The most significant velocity is along the axial direction considering the hydrodynamic problem, while the tangential and radial velocities are focal in the noise and vibration problems. The axial velocity is important

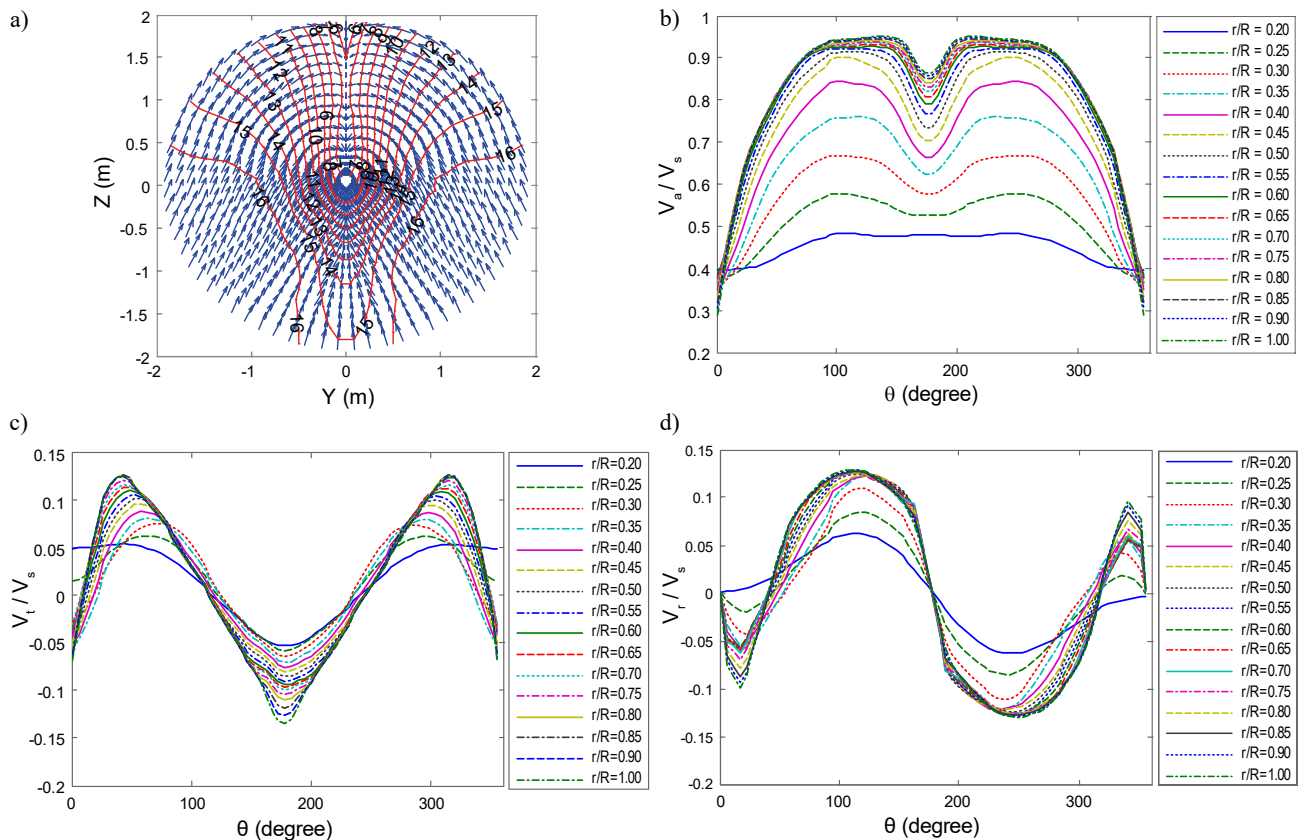


Figure 3. (a) Contour and vector velocities (b) axial, (c) tangential, and (d) radial velocity in the propeller plane at sixteen radii

in the hydrodynamic characteristics, while the other two velocities (radial and tangential) are important in terms of the vibration and cavitation problems. It means that the resultant velocity and attack angle is very important in the propeller performance under a non-uniform flow condition. The next section presents the thrust, torque, vertical and horizontal oscillating loads during one rotation for one blade and all blades during one cycle.

Results and discussions

In this section, oscillating loads are calculated with the theoretical approach discussed in the *Mathematical formulations* sections and the obtained results are analyzed. The propeller behind the ship

hull is assumed to rotate with a constant rotating speed, n , around the x -axis, in a negative direction θ , as shown in Figure 4. The results of the oscillating thrust, torque, horizontal and vertical forces are presented for one and for all the blades during one cycle, in the two following sub-sections.

Oscillating thrust and torque

A propeller produces its thrust by creating a difference between the pressures acting on the propeller blades. The oscillating inflow into the propeller blades causes dynamic changes in the blade pressure distribution. If at a point the pressure in water drops to a value equal to the vapor pressure, then cavitation occurs. If the minimum value of C_p (Eq. (11))

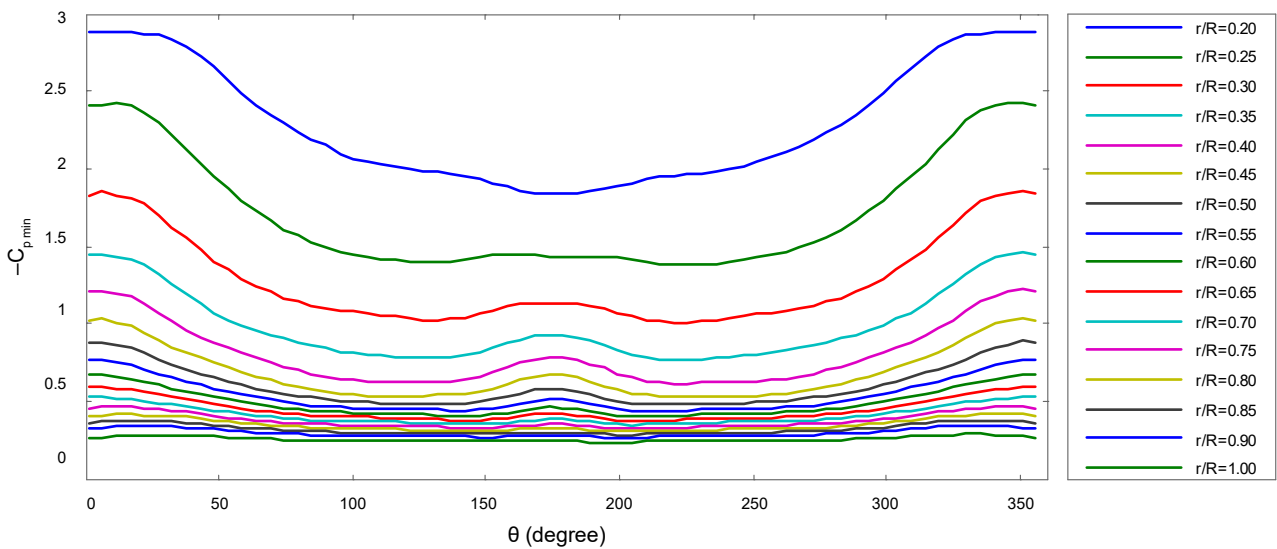


Figure 4. Minimum value of the pressure coefficient distributions at different radial sections

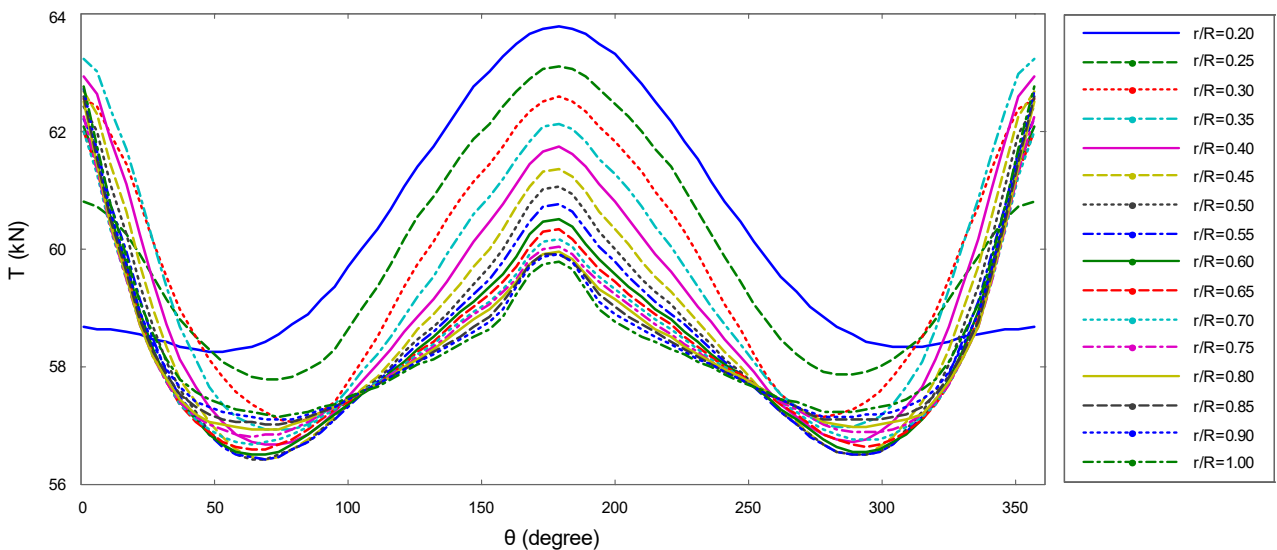


Figure 5. One blade thrust oscillating at different radial sections

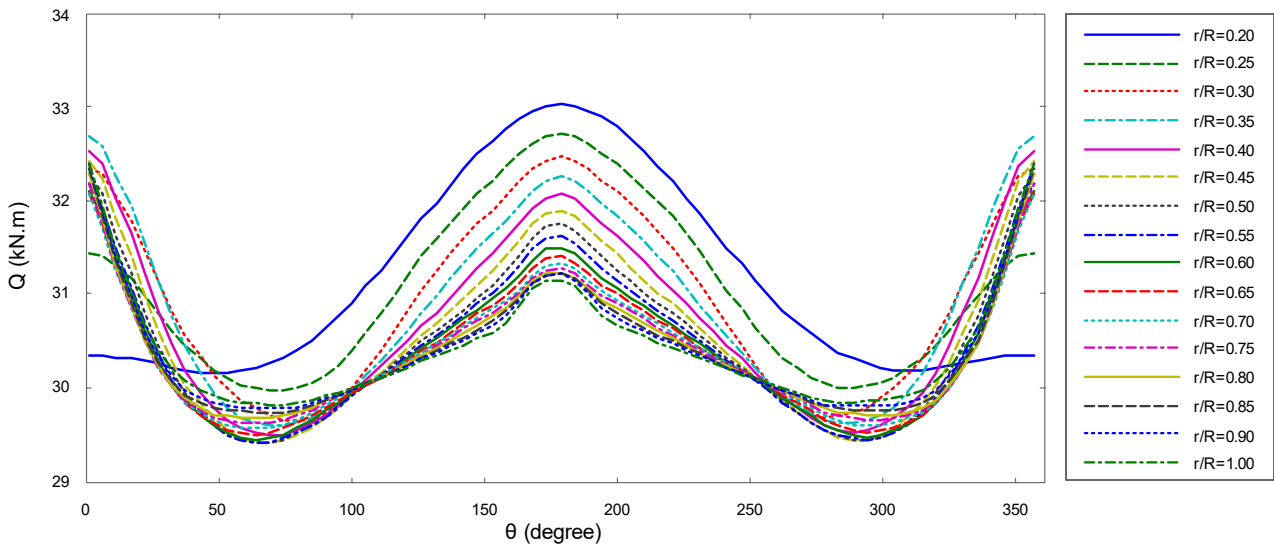


Figure 6. One blade torque oscillating at different radial sections

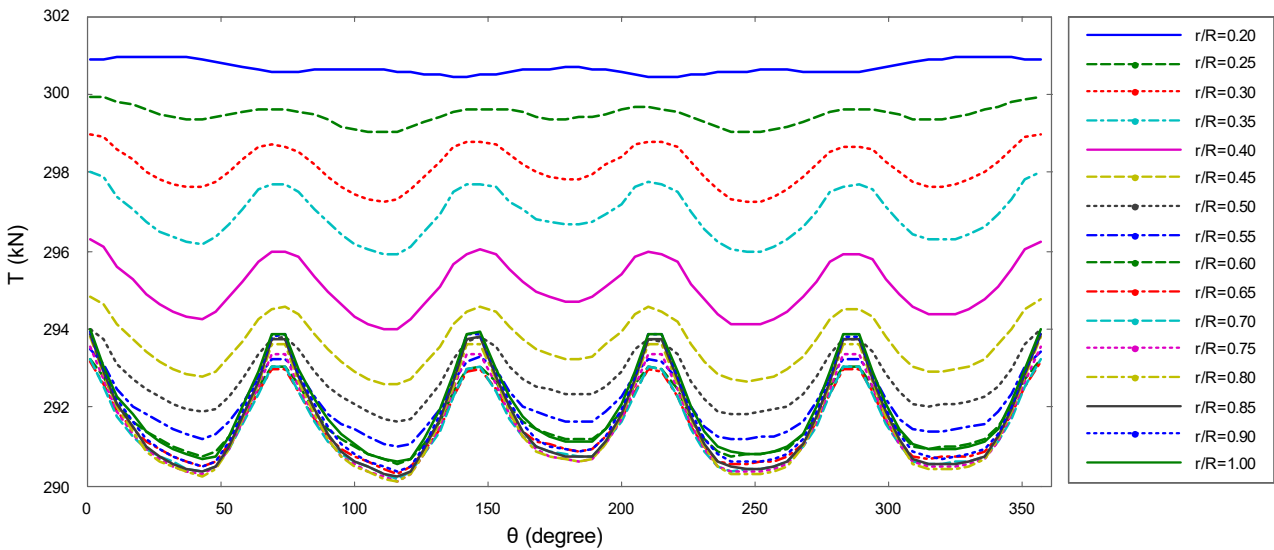


Figure 7. Oscillating thrust of all blades at different radial sections

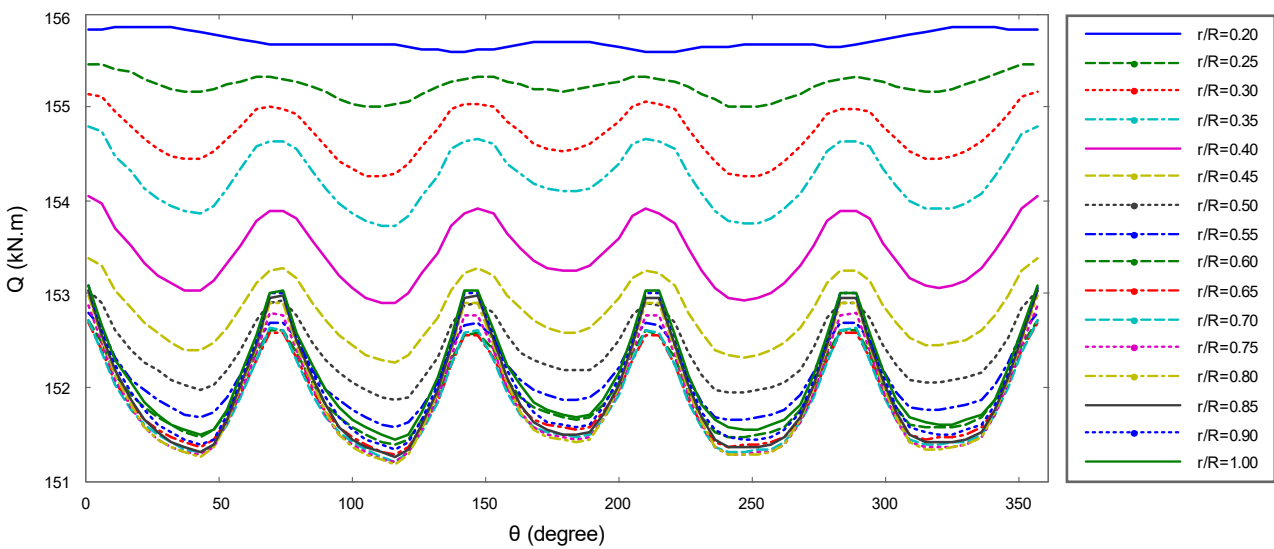


Figure 8. Oscillating torque of all blades at different radial sections

is equal to the local cavitation number, a condition for cavitation on a propeller blade section occurs. The minimum value of the pressure coefficient ($-C_{p \min}$) distributions, at angular positions of 0 to 360 degrees at different radial sections of the propeller, is presented in Figure 3. It can be concluded from this figure that with increasing radial sections, the $C_{p \min}$ decreases and therefore the probability of cavitation occurrence increases. Due to these effects, the oscillating inflow variations are investigated on the propeller to determine the thrust and torque over a single cycle. Figures 5 and 6 present the oscillating thrust and torque of the propeller at different radial sections for one blade as a function of the blade angular position (0–360 degrees) for one cycle. Variations of the thrust are achieved between 56.5 and 63.5 KN, and variations of the torque are found between 29.5 to 33 KNm. The total oscillating thrust and torque are presented in Figures 7 and 8, respectively. Higher loads and low oscillating amplitude are obtained at lower radii (near root), whilst a high amplitude is found at higher radii (near tip). Variations domain of the total thrust are 290~301 KN, and variations of total torque are around 151~156 KNm.

Oscillating horizontal and vertical forces

Oscillating loading may transmit through the propeller shafting and bearings and often produces severe vibration, noise and structural fatigue. In this subsection, the oscillating horizontal, vertical and all forces on the propeller in one cycle of the SM ship have been calculated with classical mathematical methods, discussed in section *Mathematical formulations*. The Figures 9 and 10 present one blade and an all blade forces variations for the propeller at different radial sections, as a function of the blade angular position (0–360 degrees) for a single cycle. As observed in Figure 9, one blade horizontal and vertical force variations are almost constant for different radial sections.

Conclusions

The non-uniform wake field of an SM ship was analyzed for a B-Series propeller. From the results of this study, it can be concluded that the aforementioned considered method provides a simple, fast and reliable solution, and gives oscillating load and hydrodynamic performance variations with the sufficient accuracy,

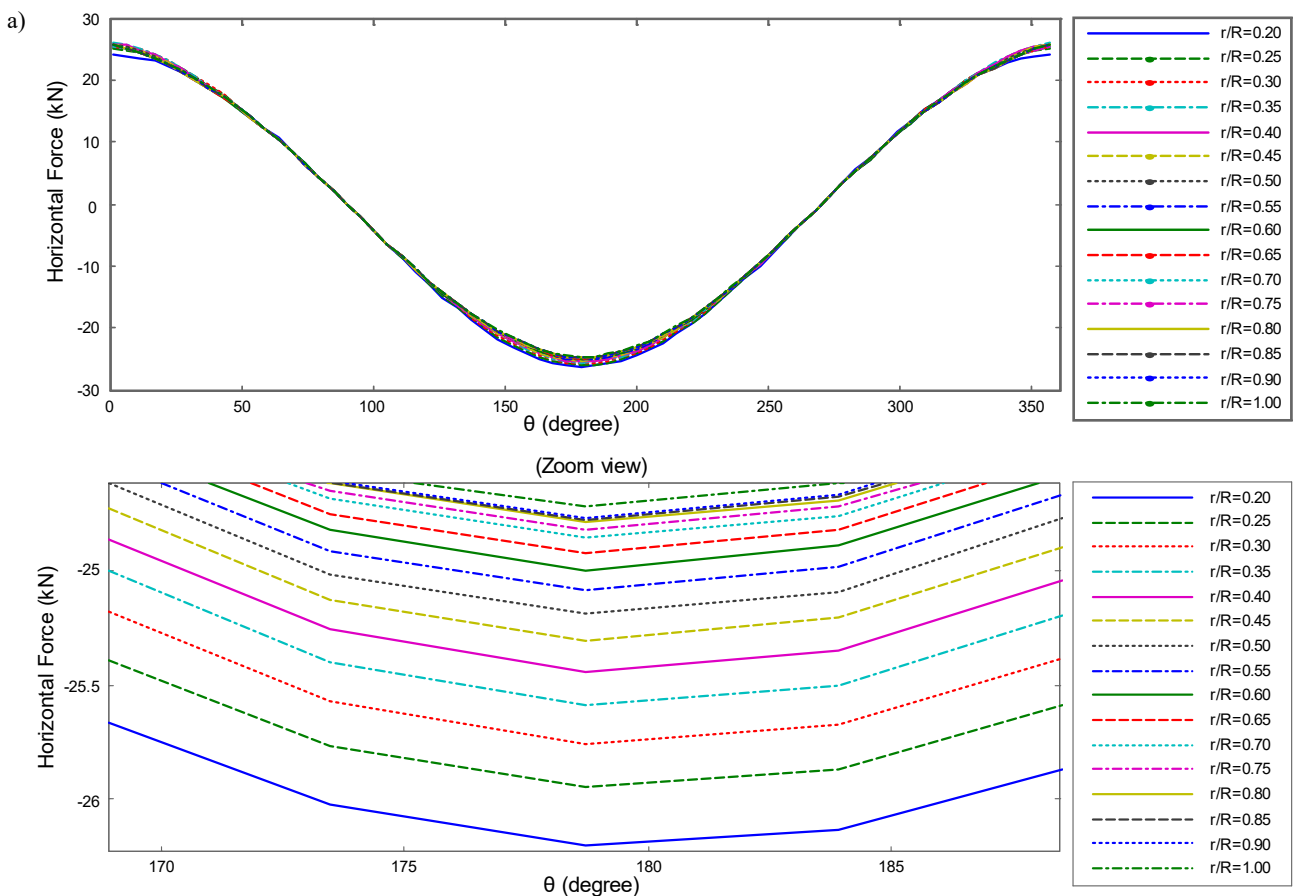


Figure 9. One blade oscillating loads including (a) horizontal force at different radial sections

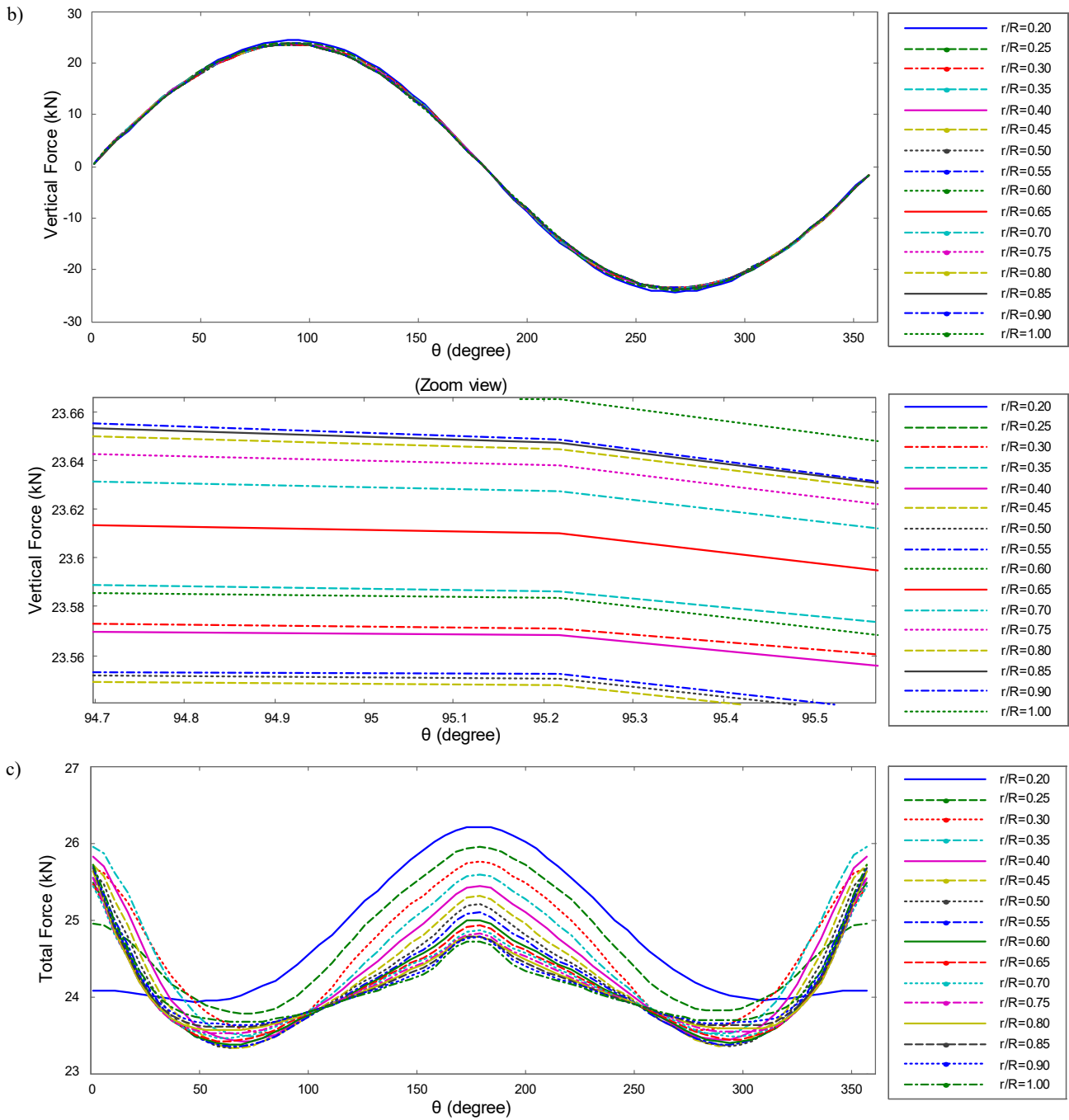


Figure 9. One blade oscillating loads including (b) vertical force, (c) total force at different radial sections

for the practical purpose of propeller pre-design. Such information is critical to the design of propulsions that can keep vibratory forces at a minimum. The main results of this study are as follows:

- Thrust and torque variations of one blade and all blades are shown in one cycle at different radial sections. A lower amplitude is found at low radial sections and a larger amplitude is obtained at high radial sections.
- With increasing radial sections, the $-C_p \min$ is decreases and therefore the probability of cavitation occurrence increases.
- Generally, the variation in thrust with the discussed parameters is the same as that shown for torque.
- The blade-frequency of the total force, thrust and torque is increased with an increase in the radial sections.
- The total force thrust and torque decrease with increasing radial blade sections and they decrease as the velocity increases.
- The presented results are useful for comparing competitive designs for the same ship and can give a good indication of which will be superior

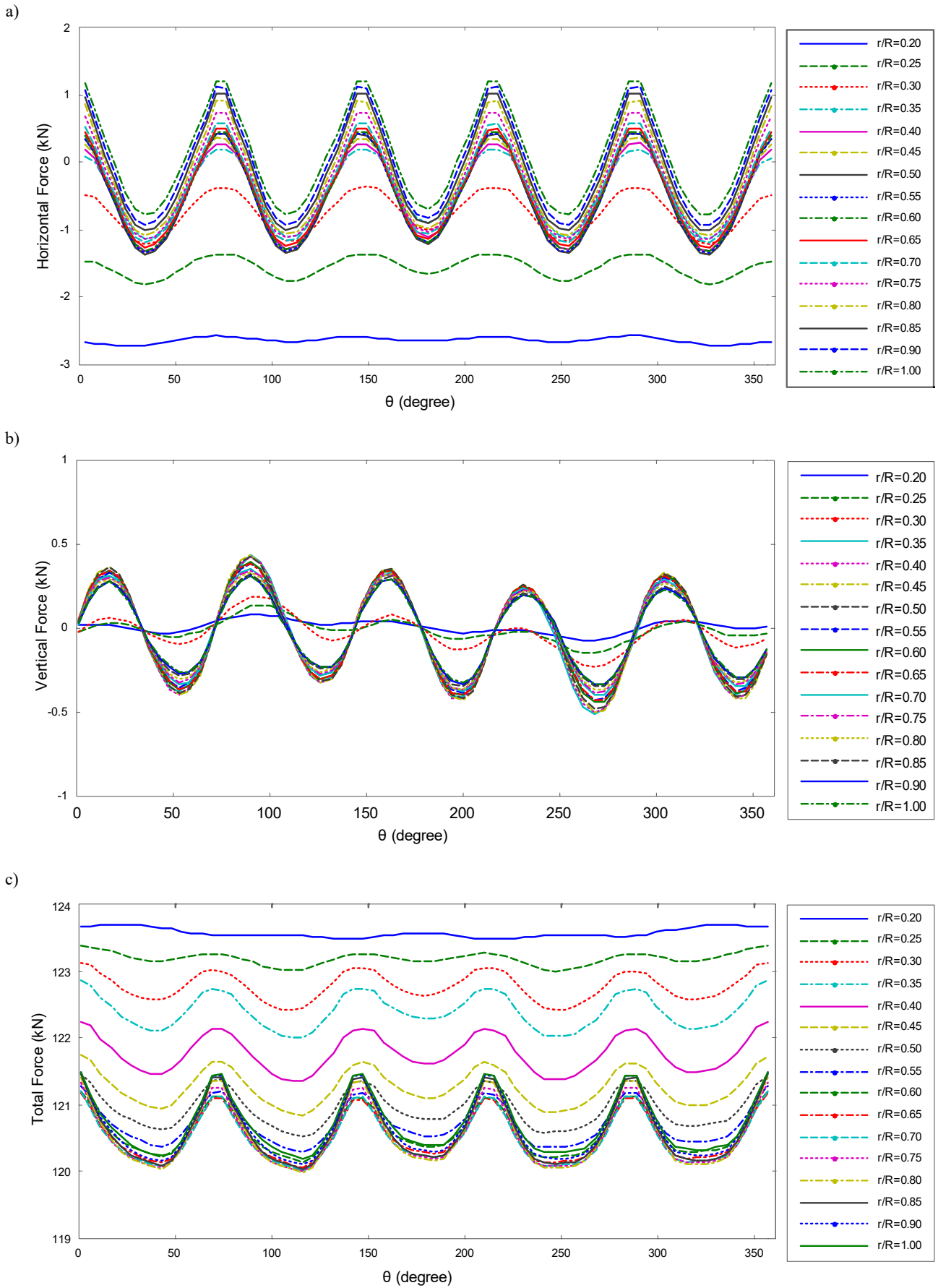


Figure 10. Oscillating loads of all blades variations including (a) horizontal force, (b) vertical force, and (c) total force at different radial sections

from a loading, vibration, cavitation and noise point of view.

The future plan is to work on the stress-strain analysis, vibration problems and dynamic motion of the propeller including the added mass, dumping coefficients and external forces generated by the shaft engine.

Acknowledgments

The publication was prepared in connection with the implementation of the project funded by the Ministry of Science and Higher Education of the Republic of Poland (grant No. 790/P-DUN/2016). The author's remuneration and costs of publication were covered by the Rector of the Maritime University of Szczecin from funds for international cooperation.

References

1. ABBAS, N., KORNEV, N., SHEVCHUK, I. & ANSCHAU, P. (2015) CFD prediction of unsteady forces on marine propellers caused by the wake nonuniformity and nonstationarity. *Ocean Engineering* 104, pp. 659–672.
2. ABRAMOWSKI, T. & SZELANGIEWICZ, T. (2009) Numerical analysis of influence of ship hull form modification on ship resistance and propulsion characteristics. Part I: Influence of hull form modification on ship resistance characteristics. *Polish Maritime Research* 4(62), 16, pp. 3–8.
3. ABRAMOWSKI, T. & SZELANGIEWICZ, T. (2010) Numerical analysis of influence of ship hull form modification on ship resistance and propulsion characteristics. Part II: Influence of hull form modification on wake current behind the ship. *Polish Maritime Research* 1(64), 17, pp. 3–9.
4. ABRAMOWSKI, T., ŻELAZNY, K. & SZELANGIEWICZ, T. (2010) Numerical analysis of influence of ship hull form modification on ship resistance and propulsion characteristics. Part III: Influence of hull form modification on screw propeller efficiency. *Polish Maritime Research* 1(64), 17, pp. 10–13.
5. ALVES PEREIRA, F., DI FELICE, F. & SALVATORE, F. (2016) Propeller cavitation in non-uniform flow and correlation with the near pressure field. *Journal of Marine Science and Engineering* 4(4), 70.
6. BERGER, S., BAUER, M., DRUCKENBROD, M. & ABDEL-MAKSOUUD, M. (2013) *Investigation of Scale Effects on Propeller-Induced Pressure Fluctuations by a Viscous/Inviscid Coupling Approach*. In Proceedings of the Third International Symposium on Marine Propulsors SMP'13, Tasmania, Australia, 5–8 May 2013, pp. 209–217.
7. CALCAGNO, G., DI FELICE, F., FELLI, M. & PEREIRA, F. (2002) *Propeller wake analysis behind a ship by stereo PIV*. 24th Symposium on Naval Hydrodynamics, Fukuoka, Japan, 8–13 July.
8. CARLTON, J.S. (2013) *Marine Propeller and Propulsion*. 3rd Ed., Butterworth-Heinemann.
9. GAAFARY, M.M., EL-KILANI, H.S. & MOUSTAFA, M.M. (2011) Optimum design of B-series marine propellers. *Alexandria Engineering Journal* 50, 1, pp. 13–18.
10. GHASSEMI, H. (2009) The effect of wake flow and skew angle on the ship propeller performance. *Scientia Iranica, Transaction B: Mechanical Engineering* 16(2), pp. 149–158.
11. GRECO, L., MUSCARI, R., TESTA, C. & DI MASCIIO, A. (2014) Marine propellers performance and flow-field prediction by a free-wake panel method. *Journal of Hydrodynamics B*, 26(5), pp. 780–795.
12. GUO, C., WU, T., ZHANG, Q., LUO, W. & SU, Y. (2017) Numerical simulation and experimental studies on aft hull local parameterized non-geosim deformation for correcting scale effects of nominal wake field. *Brodogradnja* 68(1), pp. 77–96.
13. JI, B., LUO, X., PENG, X., WU, Y. & XU, H. (2012a) Numerical analysis of cavitation evolution and excited pressure fluctuation around a propeller in non-uniform wake. *International Journal of Multiphase Flow* 43, pp. 13–21.
14. JI, B., LUO, X., WU, Y., PENG, X. & XU, H. (2012b) Partially-Averaged Navier–Stokes method with modified $k-\epsilon$ model for cavitating flow around a marine propeller in a non-uniform wake. *International Journal of Heat and Mass Transfer* 55(23), pp. 6582–6588.
15. KADOI, H., OKAMOTO, M. & SUZUKI, S. (1980) Wake distributions behind container ship models in the cavitation tunnel. *Papers of Ship Research Institute* 17(3), pp. 261–271.
16. KAMARLOUEI, M., GHASSEMI, H., ASLANSEFAT, K. & NEMATY, D. (2014) Multi-objective evolutionary optimization technique applied to propeller design. *Acta Polytechnica Hungarica* 11, 9, pp. 163–182.
17. KIM, S.Y. & MOON, B.Y. (2006) Wake distribution prediction on the propeller plane in ship design using artificial intelligence. *Ships and Offshore Structures* 1:2, pp. 89–98.
18. KLEINWÄCHTER, A., HELLMIG-RIECK, K., HEINKE, H.J. & DAMASCHKE, N.A. (2017) Full-scale total wake field PIV-measurements in comparison with ANSYS CFD calculations: a contribution to a better propeller design process. *Journal of Marine Science and Technology* 22(2), pp. 388–400.
19. KUMAR, S., NAGARAJAN, V. & SHA, O.P. (2017) Measurement of flow characteristics in propeller slipstream of a twin propeller twin rudder model ship. *International Shipbuilding Progress* 63(1–2), pp. 1–40.
20. MAHMOUDI, M., GHASSEMI, H. & NOWRUZI, H. (2018) Obtaining mathematical functions of the propeller thrust and torque coefficients fluctuations at non-uniform wake flow including geometry effects. *Mechanics & Industry* 19, 2, 205.
21. MARTIN, J.E., MICHAEL, T. & CARRICA, P.M. (2015) Submarine maneuvers using direct overset simulation of appendages and propeller and coupled CFD/potential flow propeller solver. *Journal of Ship Research* 59(1), pp. 31–48.
22. PECORARO, A., DI FELICE, F., FELLI, M., SALVATORE, F. & VIVIANI, M. (2006) *Propeller-hull interaction in a single-screw vessel*. In Proceedings of the Third International Symposium on Marine Propulsors SMP'13, Launceston, Tasmania, Australia, May 2013, pp. 185–192.
23. SHIN, K.W., REGENER, P.B. & ANDERSEN, P. (2015) *Methods for cavitation prediction on tip-modified propellers in ship wake fields*. In Proceedings of the Fourth International Symposium on Marine Propulsors SMP'15, Austin, Texas, USA, June 2015, pp. 564–571.
24. STARKE, B., WINDT, J. & RAVEN, H. (2006) *Validation of viscous flow and wake field predictions for ships at full scale*. 26th ONR Symposium on Naval Hydrodynamics, Rome, Italy, 17–22 September.

25. SUN, S., LI, L., WANG, C. & ZHANG, H. (2017) Numerical prediction analysis of propeller exciting force for hull–propeller–rudder system in oblique flow. *International Journal of Naval Architecture and Ocean Engineering* 10, 1, pp. 69–84.
26. TAHERI, R. & MAZAHERI, K. (2013) Hydrodynamic Optimization of marine propeller using gradient and non-gradient based algorithms. *Acta Polytechnica Hungarica* 10, 3, pp. 221–237.
27. UENO, M. & TSUKADA, Y. (2016) Estimation of full-scale propeller torque and thrust using free-running model ship in waves. *Ocean Engineering* 120, pp. 30–39.
28. VAZ, G., HALLY, D., HUUVA, T., BULTEN, N., MULLER, P., BECCHI, P., HERRER, J.L., WHITWORTH, S., MACÉ, R. & KORSSTRÖM, A. (2015) *Cavitating flow calculations for the E779A propeller in open water and behind conditions: code comparison and solution validation*. In Proceedings of the Fourth International Symposium on Marine Propulsors SMP'15, Austin, Texas, USA, June 2015, pp. 344–360.
29. ZOU, D., ZHANG, J., TA, N. & RAO, Z. (2017) The hydroelastic analysis of marine propellers with consideration of the effect of the shaft. *Ocean Engineering* 131, pp. 95–106.